Brain Pathology ISSN 1015-6305

RESEARCH ARTICLE

DNA Hypermethylation and Histone Modifications Downregulate the Candidate Tumor Suppressor Gene *RRP22* on 22q12 in Human Gliomas

Natalie Schmidt[1]; Sonja Windmann[1]; Guido Reifenberger[1]; Markus J. Riemenschneider[1,2]

[1] Department of Neuropathology, Heinrich Heine University, Düsseldorf.
[2] Department of Neuropathology, Regensburg University Hospital, Regensburg.

Keywords
astrocytoma, brain tumor, chromatin immunoprecipitation, glioblastoma, methylation, RASL10A.

Corresponding author:
Markus J. Riemenschneider, MD, Department of Neuropathology, Regensburg University Hospital, Franz-Josef-Strauβ-Allee 11, 93053 Regensburg, Germany (E-mail: *markus.riemenschneider@klinik.uni-regensburg.de*)

Received 14 February 2011; accepted 26 April 2011.

doi:10.1111/j.1750-3639.2011.00507.x

Abstract

RRP22 (Ras-related protein on chromosome 22) has been suggested as a candidate tumor suppressor in human cancers. Investigating a panel of 70 human gliomas, we found a frequent decrease in the *RRP22* mRNA expression levels (67%), preferentially in high-grade gliomas [World Health Organization (WHO) grades III and IV] as compared with low-grade gliomas (WHO grade II). Moreover, reduced *RRP22* mRNA expression was associated with shorter overall survival in 180 glioblastoma patients included in the National Institutes of Health Repository for Molecular Brain Neoplasia Data (NIH REMBRANDT) database. Decreased *RRP22* expression levels were in part explained by 5'-CpG island hypermethylation and increased by the treatment with the demethylating agent 5-aza-2'-deoxycytidine in glioblastoma cell lines. In addition, the *in vitro* treatment with the histone deacetylase inhibitor trichostatin A alone resulted in *RRP22* reexpression as well as a significant increase in the levels of *RRP22* promoter DNA bound to pan-acetylated histone H3 and H4. Moreover, in primary human glioblastomas, we observed an increase of H3K9me3-bound and a decrease of pan-Ac-H3-bound *RRP22* in comparison with non-neoplastic brain tissue, consistent with a heterochromatinization of the *RRP22* promoter. Taken together, our findings demonstrate that both 5'-CpG island hypermethylation and histone modifications contribute to the frequent and prognostically unfavorable transcriptional downregulation of *RRP22* in malignant gliomas.

INTRODUCTION

Ras belongs to a superfamily of small GTPases that all share pronounced sequence homologies (2, 14). While most of the Ras family members possess oncogenic properties, a number of Ras-related genes exhibit characteristics of tumor suppressors, such as the *DIRAS3* gene that is frequently hypermethylated and transcriptionally silenced in oligodendroglial tumors with 1p loss (15). A further Ras-related gene with tumor suppressor properties, which may be involved in the pathogenesis of human gliomas, is the small GTPase gene *RRP22* (Ras-related protein on chromosome 22) (21). *RRP22* (syn. *RASL10A*) was first identified in 1996 and maps to the chromosomal band 22q12, which often shows allelic losses in human tumors, including gliomas (21). Its expression appears strictly limited to the central nervous system (21). While further bibliographic data on the role of *RRP22* in human tumors is sparse (16), two studies in gliomas reported that RRP22 may suppress tumor cell growth, promote caspase-independent cell death, decrease invasiveness and inhibit glioma cell growth in soft agar, thereby supporting a tumor suppressor function (3, 4). Moreover, Chen *et al* (3) showed that the mRNA expression level decreases with increasing malignancy, and Elam *et al* (4) pointed to a role of promoter hypermethylation as a potential cause for the inactivation of *RRP22* in glioblastoma cell lines. However, the relevance of *RRP22* and its potential inactivation mechanisms in primary human glioma tissue samples *in vivo* were not investigated.

To further address the role of *RRP22* in glioma pathogenesis, we investigated primary gliomas and glioma cell lines for expression, mutation, 5'-CpG island methylation and histone modifications of *RRP22*. In addition, we used the National Institutes of Health Repository for Molecular Brain Neoplasia Data (NIH REMBRANDT) database to validate the correlation between *RRP22* gene expression, malignancy grade and patient survival. We conclude that *RRP22* is frequently downregulated in gliomas because of both aberrant promoter methylation and/or heterochromatinization, and that inactivation of *RRP22* is a negative prognostic factor in glioma patients.

MATERIALS AND METHODS

Cell lines, patients and controls

Human glioma cell lines U87MG, T98G, U138MG and A172 were obtained from the American Type Culture Collection (Manassas, VA, USA) and TP365MG cells were kindly provided by Prof V. P.

© 2011 The Authors; Brain Pathology © 2011 International Society of Neuropathology

Collins (Cambridge, UK). Tumors were selected from the archives of the Department of Neuropathology, Heinrich Heine University, Düsseldorf, Germany and investigated according to protocols approved by the institutional review board. All tumors were classified according to the criteria of the World Health Organization (WHO) 2007 classification of tumors of the nervous system (12). Parts of each tumor were snap-frozen immediately after operation and stored at −80°C. Only tissue samples with an estimated tumor cell content of 80% or more were used for molecular analyses. The tumor series was composed of the following: 70 human gliomas, including 16 primary glioblastomas, WHO grade IV (*GB*); six anaplastic astrocytomas, WHO grade III (*AA*); seven diffuse astrocytomas, WHO grade II (*A*); 11 anaplastic oligoastrocytomas, WHO grade III (*AOA*); 10 oligoastrocytomas, WHO grade II (*OA*); 12 anaplastic oligodendrogliomas, WHO grade III (*AO*); and eight oligodendrogliomas, WHO grade II (*O*) (Figure 1). For chromatin immunoprecipitation (ChIP) analyses, we additionally prepared nuclei from glioblastoma tissue specimens of seven patients (*T1–T7*, Figure 5). Five non-neoplastic brain samples from different individuals *(NB1–NB5)* were used as reference (four male, one female; median age: 69 years, age range: 43–76 years). As a positive control for the methylation studies, we used commercially available hypermethylated DNA (CpG Genome™ Universal Methylated DNA, Cat. No. S7821; Millipore, Billerica, MA).

DNA/RNA extraction

Extraction of DNA and RNA from frozen tumor tissue was performed by ultracentrifugation. In brief, tumor samples were homogenized in 6 mL 4 mol/L guanidine isothiocyanate solution. The homogenate was then layered over 4 mL CsCl and ultracentrifuged at 170 000 × g for 16 h. The RNA was recovered as a pellet and dissolved in diethylpyrocarbonate-treated water containing the RNase inhibitor RNasin (Promega, Madison, WI). The DNA was purified from the CsCl phase using proteinase K digestion followed by phenol/chloroform extraction. Total DNA and RNA extraction from cell culture and peripheral blood leukocytes was performed according to a standard protocol.

Real-time reverse transcription (RT) PCR analysis

Three micrograms of total RNA from each tumor or cell line were reverse transcribed into cDNA with superscript reverse transcriptase (Invitrogen, Carlsbad, CA). Expression of *RRP22* transcripts was determined by SybrGreen-based real-time PCR using the StepOnePlus™ sequence detection system (Applied Biosystems, Foster City, CA) as previously described (1). Fold expression changes relative to non-neoplastic brain tissue were calculated with the ΔΔCT method (11) using *ARF1* (ADP-ribosylation factor 1) as the reference transcript (for primer sequences, see Supporting Table S1).

Microsatellite analysis

Peripheral blood samples were available from 47 of the 70 patients. To investigate the respective tumors for allelic losses spanning the *RRP22* locus on 22q12, we employed loss of heterozygosity (LOH) analysis at the following four microsatellite markers [nucleotide (nt) numbering according to the University of California, Santa Cruz (UCSC) genome browser at http://www.genome.ucsc.edu, primers supplied in Supporting Table S1]: *D22S1176* (nt 32 226 567–32 226 714) and *D22S531* (nt 30 699 219–30 699 650) located telomerically as well as *D22S1150* (nt 29 501 326–29 501 658) and *D22S689* (nt 28 856 340–28 856 833) located centromerically to *RRP22* (nt 29 708 923–29 711 748).

Mutational analysis

Single-strand conformation polymorphism (SSCP)/heteroduplex analysis was performed to screen for mutations in the *RRP22* coding sequences. In brief, PCR products (primer sequences listed in Supporting Table S1) were separated by electrophoresis on 10%–12% non-denaturing polyacrylamide gels at room temperature and at 4°C. After electrophoresis, the SSCP/heteroduplex band patterns were visualized by silver staining of the gels. In case of aberrant band patterns, PCR products were sequenced using the BigDye Cycle Sequencing Kit and an ABI PRISM 377 semi-automated DNA sequencer (Applied Biosystems, Foster City, CA).

Methylation analysis using sodium bisulfite sequencing

Sodium bisulfite treatment of 1 µg DNA was performed overnight (16 h) according to a standard protocol (13). PCR fragments were then amplified from sodium bisulfite-modified DNA using the primers as reported in Supporting Table S1. The amplified fragment of the *RRP22* 5′-CpG island covered a total of 36 CpG sites (nt 29 711 182–29 711 416 according to UCSC, CpGs +53 to +88 relative to the transcription start site), and for 24 of these CpG sites overlapped with a region that had been shown to be methylated in glioblastoma cell lines (4). Direct sequencing and semiquantitative calculation of a promoter methylation score were carried out as described (19). In short, the methylation status at each of the analyzed CpG sites was rated using the following scale: 0, completely unmethylated; 1, a weak methylated signal detectable in the sequence; 2, methylated signal approximately equal to unmethylated signal; 3, methylated signal markedly stronger than unmethylated signal. Based on this rating, a cumulative promoter methylation score was calculated for each tumor. Tumors with methylation scores exceeding that of non-neoplastic brain tissue were regarded as hypermethylated.

5-Aza-2′-deoxycytidine (AZA) and trichostatin A (TSA) treatment of malignant glioma cell lines

Two glioma cell lines (A172 and U87MG) were grown under standard conditions or under two different treatment conditions with either the demethylating agent AZA (1 µM for 72 h, *AZA*) or the histone deacetylase inhibitor TSA (1 µM for 36 h, *TSA*). After harvesting the cells and extracting the mRNA, expression of *RRP22* transcripts under the different treatment conditions compared with the untreated controls was assessed by real-time reverse transcription PCR analysis as described earlier (Figure 3). Results obtained were reproduced in at least three independent biological experiments.

© 2011 The Authors; Brain Pathology © 2011 International Society of Neuropathology

Chromatin immunoprecipitation (ChIP) assays

ChIP was performed from TSA-treated glioblastoma cells as well as from fresh frozen glioblastoma tissues. DNA and proteins were cross-linked with 1% formaldehyde for 10 minutes and then resuspended in swelling buffer to isolate nuclei. Purification of nuclei from fresh frozen tissues was accomplished via sucrose gradient ultracentrifugation as described (9). Shortly, frozen tissues were homogenized by douncing in nuclear extraction buffer, nuclei were then fixed by adding 1% formaldehyde for 10 minutes and the tissue homogenates transferred on top of a sucrose cushion and ultracentrifuged at 25 000 rpm for 3 h at 4°C (SW41 Ti Rotor, Beckman Coulter).

Nuclei prepared from cells or tumor tissues were further processed using a commercial ChIP assay kit (Upstate, Charlottesville, VA) according to the manufacturer's recommendations. After resuspension in SDS-lysis buffer, genomic DNA was sheared to 200–800 bp fragments by sonication with an ultrasonic processor (Vibracell 75022; Novodirect, Kehl, Germany). Sonicated samples were then precleared with protein A agarose/salmon sperm DNA (Upstate) for 30 minutes at 4°C to reduce nonspecific binding. A 5% sample volume was saved as input control while the rest was used for immunoprecipitation at 4°C overnight. In case of cell lines, immunoprecipitation was performed with anti-H3ac and anti-H4ac antibodies (Figure 4). In the tumors, we employed antibodies against H3ac and H3K9me3 (Figure 5) for immunoprecipitation. In both assays, rabbit antihuman IgG fraction served as a negative isotype control (all antibodies from Upstate). Antibody/histone/DNA complexes were collected using protein A agarose/salmon sperm DNA (1 h at 4°C) and the histone/DNA complexes were then eluted from the antibodies (2 × 15 minutes. incubation at room temperature in freshly prepared elution buffer). After reversing the histone–DNA crosslink (NaCl for 4–6 h at 65°C), the DNA was extracted by a standard proteinase K digest and subsequent phenol/chloroform extraction.

Immunoprecipitated DNA was assessed by using real-time PCR analysis with primers targeting the promoter sequences of *RRP22* and normalized to the respective input fraction as a reference. *GAPDH* was used as a negative control gene associated with euchromatin and not regulated by histone modifications. *p21* served as a positive control gene previously shown to be inactivated by histone modifications in human glioblastoma cells (20) (for primers, compare Supporting Table S1). Results obtained from glioblastoma cells were reproduced in three independent biological experiments. For fresh frozen glioblastoma tissues, the results are based on the measurement of three technical replicates caused by the restricted amount of immunoprecipitated DNA. Tricine-SDS-PAGE (17) was performed to control for the efficacy of TSA treatment and the specificity of ChIP antibody reactions (data not shown).

Assessment of the prognostic role of *RRP22* in the NIH REMBRANDT database

The NIH REMBRANDT database (URL: https://caintegrator.nci.nih.gov/rembrandt/home.do) was used to correlate *RRP22* gene expression with tumor malignancy grade as well as patient overall survival (Kaplan–Meier survival plot for *RRP22* gene expression in gliomas of different WHO grades as well as glioblastomas of WHO grade IV; Figure 6). Patients were divided into three groups based on the *RRP22* expression levels (high, ≥twofold; intermediate, 0.5–twofold; and low, ≤0.5-fold compared with non-neoplastic brain tissue) using the means of all probe sets annotated for *RRP22* (Figure 6). The log rank *P*-value was calculated using the Mantel–Haenszel algorithm and indicated the significance of survival differences between any two groups of samples segregated based on *RRP22* gene expression.

Assessment of other molecular alterations common in gliomas

Microsatellite analyses were used to assess the allelic status on chromosome arms 1p (microsatellite markers D1S211, D1S468, D1S507, D1S2629) and 19q (microsatellite markers D19S572, D19S1182, D19S210 and D19S219) as reported elsewhere (5). *IDH1* and *IDH2* mutational status was assessed by pyrosequencing as previously described (7). *IDH2* mutations were only assessed in case of the detection of a wild-type sequence for *IDH1*. p53 protein expression was assessed by immunohistochemistry (clone DO-7; Dako, Hamburg, Germany) scoring nuclear staining with the following semiquantitative score: 0, no immunopositive tumor cells; 1, <10%; 2, 10%–49%; 3, 50%–90%; and 4, >90% tumor cells with immunopositive nuclei.

Statistical methods

Two-sided Student's *t*-test analyses were employed to compare *RRP22* mRNA expression levels between the different WHO grades and to compare *RRP22* mRNA expression levels between tumors with and without *RRP22* 5′-CpG island hypermethylation (relative to non-neoplastic brain tissue). One-sided Student's *t*-test analyses were used to evaluate the increase of *RRP22* expression levels in glioblastoma cell lines after treatment with AZA and TSA. One-sided Student's *t*-test analyses were also used to assess the increase of *RRP22* immunoprecipitated DNA bound to acetylated histones after TSA treatment. *P*-values of <0.05 (*), <0.01 (**) and <0.001 (***) were considered as significant. For the correlation of the *RRP22* promoter methylation status with *IDH1* and *IDH2* mutations as well as with the allelic status on 1p and 19q, we used two-tailed Fisher's exact test. Correlation between the *RRP22* promoter methylation status and the p53 protein expression score was assessed by using Mann–Whitney *U*-test analysis.

RESULTS

RRP22 is transcriptionally downregulated in the majority of the investigated gliomas

When investigating a series of 70 glioma patients by means of real-time reverse transcription PCR analysis, we found decreased *RRP22* mRNA levels (<0.7-fold relative to non-neoplastic brain tissue) in 47 out of 70 gliomas (67%) (Figure 1). Interestingly, when comparing *RRP22* expression levels between the different WHO grades, *RRP22* expression decreased with higher malignancy grade. Highest *RRP22* expression levels were observed in WHO grade II lesions (mean: 1.7; standard deviation, SD: 1.7), intermediate expression levels in WHO grade III gliomas (mean: 0.8; SD: 1.4) and lowest expression levels in glioblastomas of WHO grade IV

© 2011 The Authors; Brain Pathology © 2011 International Society of Neuropathology

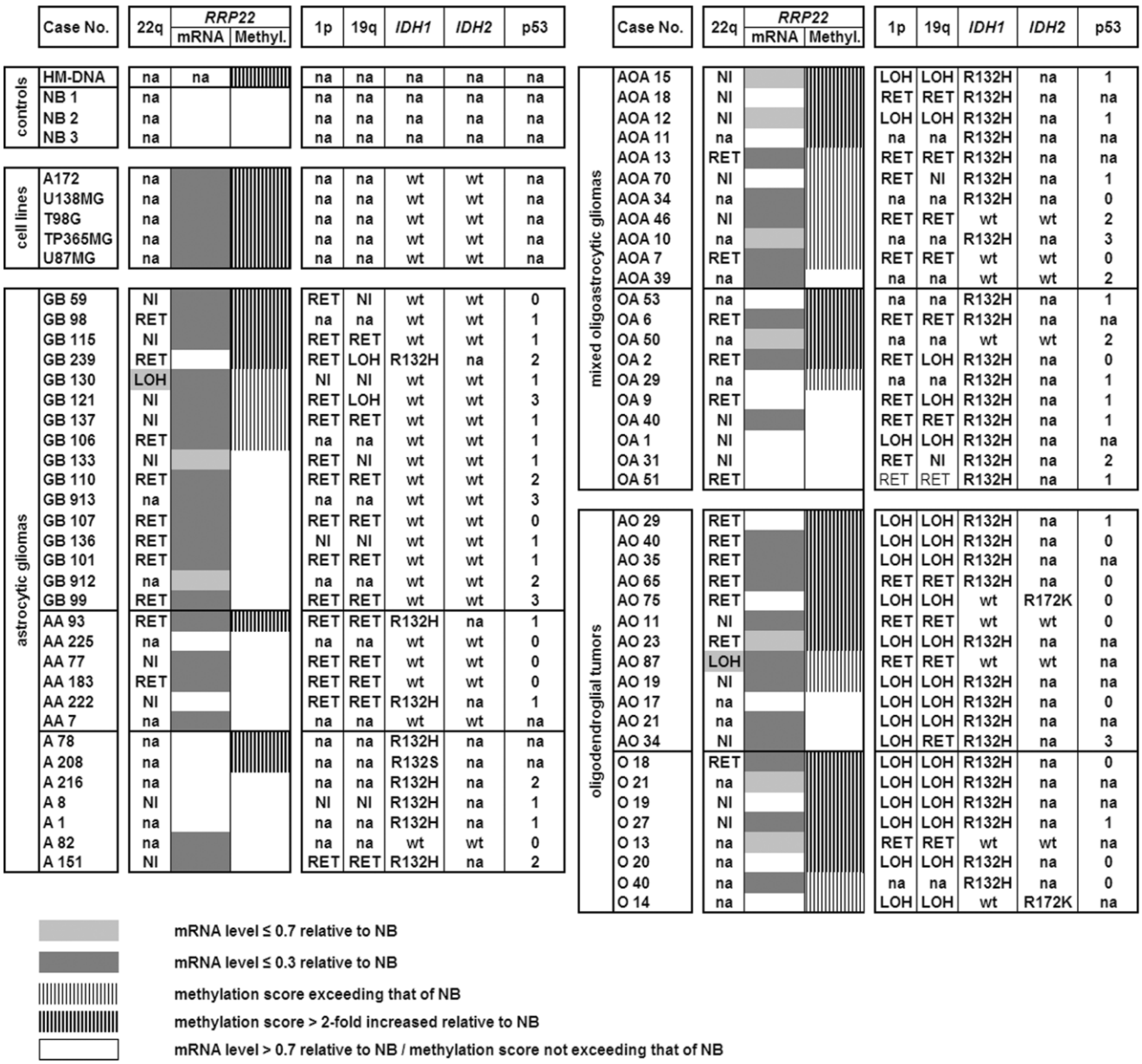

Figure 1. Molecular genetic aberrations of *RRP22* in synopsis with other common molecular alterations in human gliomas. Note that *RRP22* transcript levels (*mRNA*) are decreased relative to non-neoplastic brain tissue in all glioblastoma cell lines and the majority of the investigated tumors. Transcriptional downregulation of *RRP22* is only, in part, explained by *RRP22* 5′-CpG island hypermethylation (*methyl.*). *NB1-3*, 3 different samples of non-neoplastic brain tissue; *HM-DNA*, *in vitro* hypermethylated DNA control; *LOH*, loss of heterozygosity on 22q12 spanning the *RRP22* locus), 1p and 19q as assessed by microsatellite analyses; *RET*, retention of heterozygosity at all investigated informative loci on these chromosomal arms; *NI*, not informative at the investigated loci; *na*, not analyzed. *IDH1/2* mutations were assessed by pyrosequencing (*wt*, wild-type sequence) and p53 protein expression by semiquantitative immunohistochemistry (0, no immunopositive tumor cells; 1, <10%; 2, 10%–49%; 3, 50%–90% and 4, >90% tumor cells with immunopositive nuclei).

(mean: 0.3; SD: 0.8). The expression differences between the grades were statistically significant, particularly when comparing high-grade (malignant) gliomas (WHO grade III and IV) with low-grade gliomas of WHO grade II (Student's *t*-test, $P = 0.003$; Figure 2A). All five investigated glioblastoma cell lines (A172, U138MG, T98G, TP365MG and U87MG) exhibited a nearly complete loss of expression (<0.1) of *RRP22* transcripts (Figure 1).

Lack of detectable *RRP22* mutations and low frequencies of allelic deletions on 22q12

Mutational analysis of the entire coding regions of *RRP22* by SSCP/heteroduplex analysis did not detect somatic mutations in any of the 70 gliomas (data not shown). As *RRP22* is located in a chromosomal region that is often affected by allelic losses in

© 2011 The Authors; Brain Pathology © 2011 International Society of Neuropathology

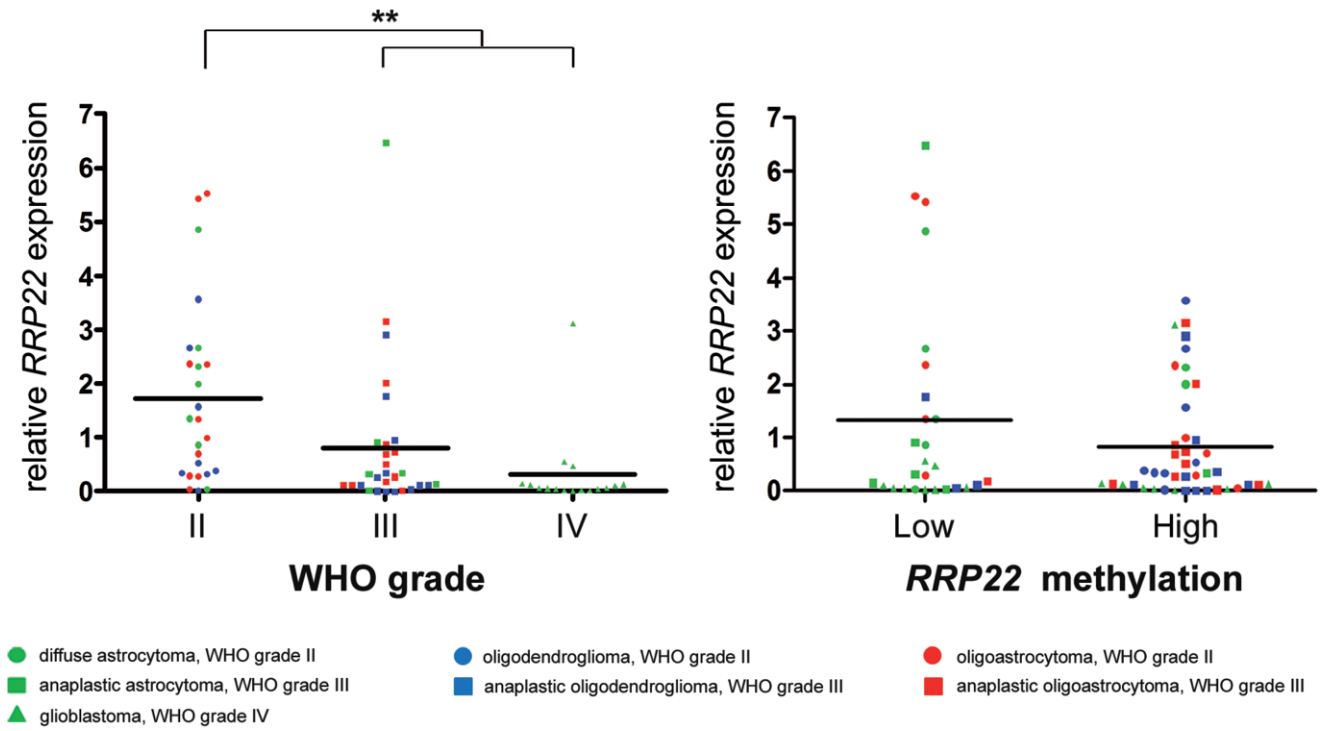

Figure 2. *RRP22* mRNA expression in human gliomas stratified for WHO grade and methylation status. Note that *RRP22* mRNA expression is significantly decreased in high-grade (WHO grade III and IV) as compared with low-grade (WHO grade II) gliomas (**A**). Tumors with increased *RRP22* 5′-CpG island methylation scores (relative to that of non-neoplastic brain tissue) had a lower mean *RRP22* mRNA expression level (0.8) as compared with tumors with absent or low *RRP22* methylation (1.3); however, these expression differences missed the significance threshold (**B**).

human tumors, including gliomas (8), we analyzed a set of microsatellite markers spanning the *RRP22* locus on 22q12 and identified two patients (GB130, AO87) with allelic losses in the tumor tissue (Figure 1). Both patients with *RRP22* allelic deletions exhibited 5′-CpG island hypermethylation of the second allele (see later) resulting in strongly decreased *RRP22* mRNA expression levels of 0.1 relative to non-neoplastic brain tissue.

Hypermethylation of the *RRP22* 5′-CpG island partially accounts for the downregulation of *RRP22* expression in human gliomas

Direct bisulfite sequencing revealed *RRP22* 5′-CpG island hypermethylation in 43 out of 70 glioma patients (61%) and in all five investigated glioblastoma cell lines. *In vitro* treatment with the demethylating agent 5-aza-2′-deoxycytidine induced a significant increase of *RRPP2* transcripts in two selected glioblastoma cell lines (A172: fourfold, $P = 0.013$; U87MG: 11-fold, $P = 0.003$) relative to untreated control cells (*CTRL*), thus corroborating a causal relationship between *RRP22* 5′-CpG island methylation and mRNA expression (Figure 3). In the primary gliomas, we found lower mean *RRP22* mRNA expression levels in tumors with increased *RRP22* methylation (mean: 0.8; SD: 1.1) compared with tumors with low or absent *RRP22* methylation (mean: 1.3; SD: 2.0). However, these expression differences did not reach statistical significance (Student's *t*-test, $P = 0.15$; Figure 2B) and only 30 out

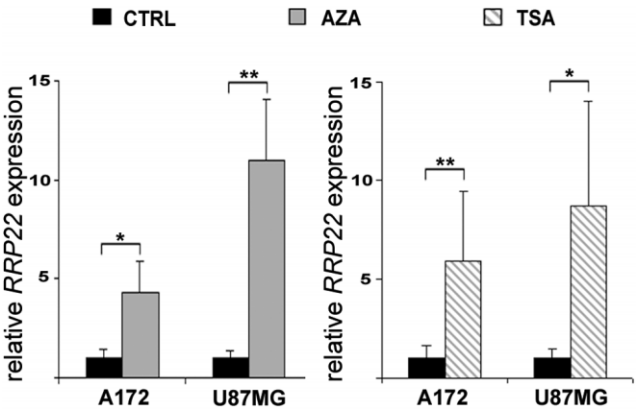

Figure 3. Increased expression of *RRP22* transcripts in human malignant glioma cell lines A172 and U87MG after treatment with 5-aza-2′-deoxycytidine (AZA) or trichostatin A (TSA). Real-time RT-PCR analysis shows increased expression of *RRP22* transcripts relative to the untreated control (*CTRL*, cells grown under standard conditions) both when applying AZA or TSA. These findings corroborate a causal relationship between *RRP22* promoter hypermethylation and decreased mRNA expression but also suggest histone modifications as an additional cause of *RRP22* downregulation in glioma cells.

© 2011 The Authors; Brain Pathology © 2011 International Society of Neuropathology

of the 47 gliomas with decreased *RRP22* expression demonstrated a concomitant 5′-CpG island hypermethylation, suggesting that additional mechanisms contribute to the reduced expression of *RRP22* in a subgroup of human gliomas.

In vitro treatment of glioblastoma cell lines with the histone deacetylase inhibitor TSA suggests a role for histone modifications in *RRP22* downregulation

We then treated two glioblastoma cell lines (A172 and U87MG) with the histone deacetylase inhibitor TSA. Relative to the untreated controls, we found a significant mRNA expression increase for both genes in A172 (*RRP22*: sixfold, $P = 0.004$) and U87MG (*RRP22*: ninefold, $P = 0.013$) glioblastoma cells (Figure 3). Consequently, we next employed ChIP analyses in the same two cell lines to assess a potential euchromatinization of the *RRP22* promoter after TSA treatment. Quantitative real-time PCR analysis following ChIP analysis revealed a significant increase of *RRP22* promoter DNA bound to acetylated H3 (H3ac; 23-fold for U87MG, $P = 0.0002$; and 13-fold for A172, $P = 0.0007$) and H4 (H4ac; 16-fold for U87MG, $P = 0.002$; and 10-fold for A172, $P = 0.0003$) when comparing TSA-treated and untreated cells (Figure 4).

ChIP confirms heterochromatinization of the *RRP22* promoter in a fraction of primary glioblastomas

To further address the relevance of histone modifications for the regulation of *RRP22* in primary glioblastoma tissues, we optimized our ChIP protocol for the use on tissue samples and prepared the chromatin of three non-neoplastic brain tissues (*NB1, 4 and 5*) and seven glioblastomas (*T1–T7*, Figure 5). With antibodies against acetylated histone H3 (associated with euchromatin) and histone H3 trimethylated at lysine residue 9 (H3K9me3, which is associated with heterochromatin), we found that in the three non-neoplastic brain tissues, the ratio between H3ac- and H3K9me3-bound DNA invariably exceeded one, indicating a prevailing euchromatic stage of the H3-bound *RRP22* promoter (Figure 5). A similar euchromatic pattern was observed for the promoter of the control gene *GAPDH* (data not shown) in the non-neoplastic tissue samples as well as in all investigated tumors. For *RRP22*, in contrast, three out of the seven investigated glioblastomas (*T2*, *T3* and *T4*) exhibited a shift toward heterochromatinization of the H3-bound *RRP22* promoter (ratio H3ac/H3K9me3 <1, Figure 5A, ▼) in comparison with non-neoplastic brain tissue, thus indicating promoter inactivation by histone modifications. Notably, heterochromatinization of the *RRP22* promoter was observed alone (two

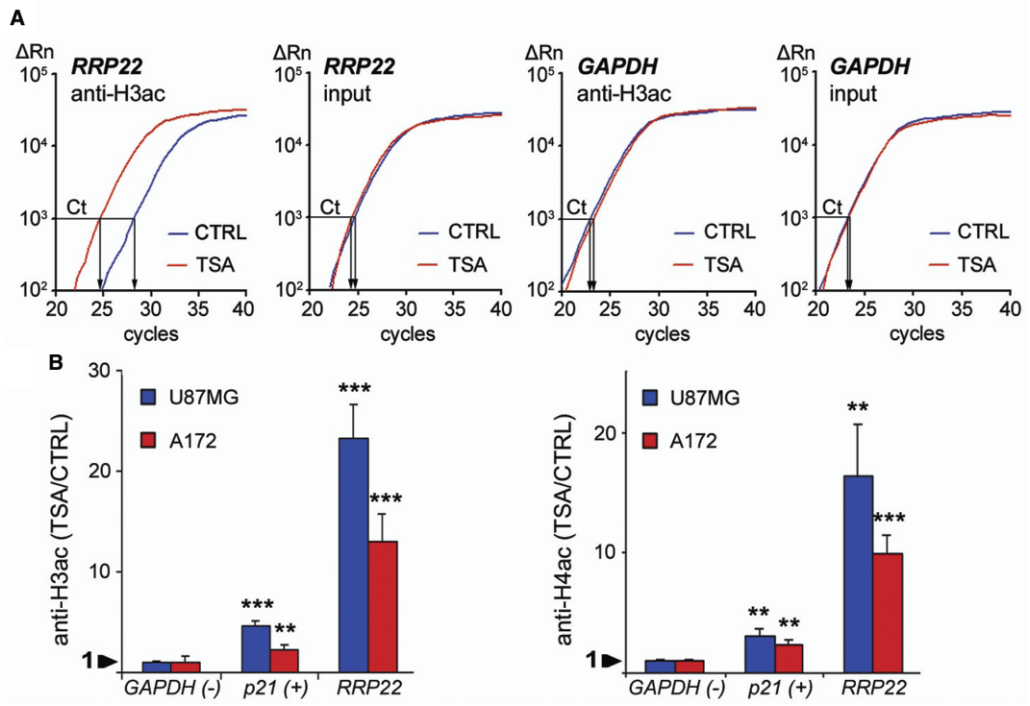

Figure 4. *In vitro* treatment with the histone deactylase inhibitor trichostatin A (TSA) causes euchromatinization of the *RRP22* promoter in the glioblastoma cell lines U87MG and A172. Quantitative real-time PCR analysis of *RRP22* promoter DNA binding to anti-H3ac and anti-H4ac after euchromatinizing treatment with TSA. (**A**) Note that in the glioblastoma cell line, A172 the TSA (*red*) curve for anti-H3ac-bound *RRP22* is shifted to the left relative to the CTRL (*blue*) curve, while the reference curves (*input*) for TSA and CTRL pass the threshold (*Ct*) at an approximately equal cycle number. This corresponds to markedly increased *RRP22* promoter DNA levels bound to H3ac after treatment with TSA. *Abscissa*, cycle number; *ordinate*, relative amount of PCR product. (**B**) After TSA treatment, an increase of promoter DNA binding of *RRP22* to H3ac (*left*) and H4ac (*right*) is observed in both cell lines (ratio TSA/CTRL >1). *p21*, positive control gene (*CDKN1A/p21*^{WAF1}) known to be inactivated by histone modifications in gliomas; *GAPDH*, negative control gene not regulated by histone modifications.

© 2011 The Authors; Brain Pathology © 2011 International Society of Neuropathology

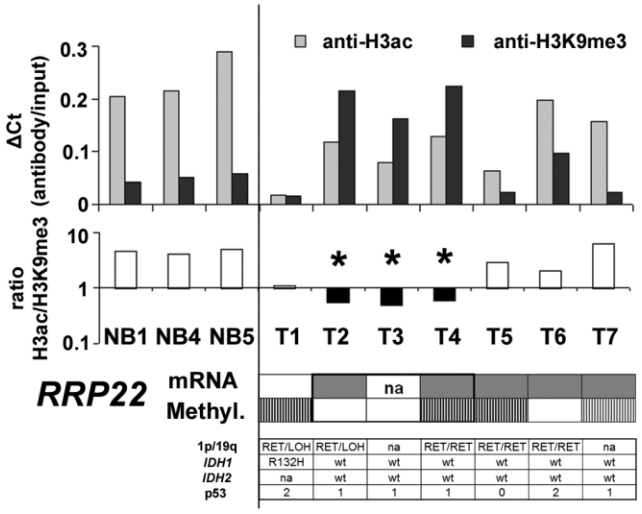

Figure 5. Chromatin immunoprecipitation confirms heterochromatinization of the *RRP22* promoter in human glioma tissues. Shown are ΔCt values (antibody/input) for chromatin immunoprecipitation with antibodies against H3ac (associated with euchromatin) and H3K9me3 (associated with heterochromatin) as well as the H3ac/H3K9me3 ratios for three different non-neoplastic brain tissues (NB1, 4, 5) and seven glioblastomas. The numbers correspond to: *T1*, GB239; *T2*, GB1060; *T3*, GB1061; *T4*, GB1062; *T5*, GB1063; *T6*, GB1064; *T7*, GB1065. Note that in non-neoplastic brain tissues, the ratio between anti-H3ac and anti-H3K9me3 is invariably exceeding 1, indicating a prevailing euchromatic stage of the H3-bound promoters. Three glioblastomas (*T2, T3* and *T4*) show a shift toward a heterochromatinization of H3-bound *RRP22* promoter DNA (ratio H3ac/H3K9me3 <1, ▼). One of these three patients has a concomitant *RRP22* hypermethylation, while the other two patients lack *RRP22* methylation indicating that histone modifications together with promoter hypermethylation or alone contribute to the frequent transcriptional downregulation of *RRP22* in human gliomas (color-code for visualization of mRNA expression and methylation status is the same as introduced in Figure 1). Also shown is the allelic status on 1p and 19q, the mutational status of *IDH1* and *IDH2* as well as the p53 protein expression score for all seven glioblastomas.

out of three patients) as well as in conjunction with *RRP22* hypermethylation (one out of three patients), and *RRP22* mRNA expression was strongly decreased in both of these settings (Figure 5).

Correlation of *RRP22* gene expression data to tumor malignancy grade and patient overall survival in the NIH REMBRANDT database

Our experimental findings of a decreased *RRP22* expression with higher malignancy grade can be retraced in the NIH REMBRANDT data set (data not shown). More interestingly, correlation of *RRP22* expression and patient survival revealed a longer overall survival for patients with increased *RRP22* expression (Figure 6). A total of 343 patients with diffusely infiltrating gliomas of different WHO grades were divided into three groups according to *RRP22* mRNA expression relative to non-neoplastic brain tissue (high, intermediate and low *RRP22* expression levels). The NIH REMBRANDT database reveals significant differences when comparing the group of tumors with low *RRP22* transcript levels (213 patients, median overall survival: 456 days) with tumors with high *RRP22* expression (17 patients, median overall survival: 2004 days; log-rank test: $P = 5.95 \times 10^{-5}$; Figure 6A) as well as with tumors with intermediate *RRP22* transcript levels (113 patients; median overall survival: 1137 days; log-rank test: $P = 1.27 \times 10^{-8}$; Figure 6A). In addition, in a cohort of 180 glioblastoma patients (WHO grade IV), individuals with intermediate *RRP22* expression (35 patients; median survival: 666 days) exhibited a significantly better overall survival than patients with low *RRP22* expression levels (145 patients; median overall survival: 396 days; log-rank test: $P = 0.005$; Figure 6B). As the group of glioblastoma patients with a high *RRP22* expression was composed of only a single individual, it was not usable for meaningful statistical comparisons.

Correlation of *RRP22* epigenetic inactivation with other molecular alterations common in gliomas

We correlated the *RRP22* methylation status in our tumor panel to other common molecular alterations in gliomas, namely *IDH1* and *IDH2* mutations, allelic losses on chromosome arms 1p and 19q and p53 protein expression (results for the individual tumors are shown in Figure 1). For the microsatellite analyses on 1p and 19q, we were restricted to the patients from whom we had peripheral blood samples available (51 out of 70 patients of our tumor panel). None of the assessed correlations proved statistically significant (*RRP22* promoter methylation status vs. *IDH1/2* mutations, Fisher's exact test, $P = 0.08$; vs. 1p deletions, Fisher's exact test, $P = 0.21$; vs. 19q deletions, Fisher's exact test, $P = 0.06$; vs. 1p/19q deletions, Fisher's exact test, $P = 0.09$; vs. p53 protein expression, Mann–Whitney *U*-test, $P = 0.14$). Also, the three out of the seven glioblastomas with histone modifications impacting *RRP22* did not exhibit a strikingly unique pattern of associated molecular alterations (Figure 5). Here, statistical analyses were not performed because of the restricted number of tumors analyzed by the ChIP method.

DISCUSSION

The RAS-related gene *RRP22* has been suggested as a tumor suppressor in glioma cells (3, 4), but its relevance and inactivation mechanisms in glioma patient samples had not been fully assessed so far. We performed a comprehensive molecular analysis of *RRP22* in a panel of 70 human gliomas and found a frequent reduction of *RRP22* (67%) transcript levels. *RRP22* mRNA expression levels were significantly decreased in high-grade (WHO grade III and IV) as compared with low-grade (WHO grade II) gliomas. These findings are in accordance with a recently published report on *RRP22* transcriptional downregulation with increasing WHO grade in astrocytomas (3).

RRP22 methylation analysis by means of direct bisulfite sequencing revealed hypermethylation of the *RRP22* 5′-CpG island in a subset of gliomas with decreased *RRP22* mRNA expression levels. This finding is in line with a previous report on hypermethylation of *RRP22* in selected immortalized glioblastoma cell lines (4). Furthermore, when treating A172 and U87MG glioblastoma cell lines with the demethylating agent 5-aza-2′-deoxycytidine *in vitro*, we found a significant increase in

© 2011 The Authors; Brain Pathology © 2011 International Society of Neuropathology

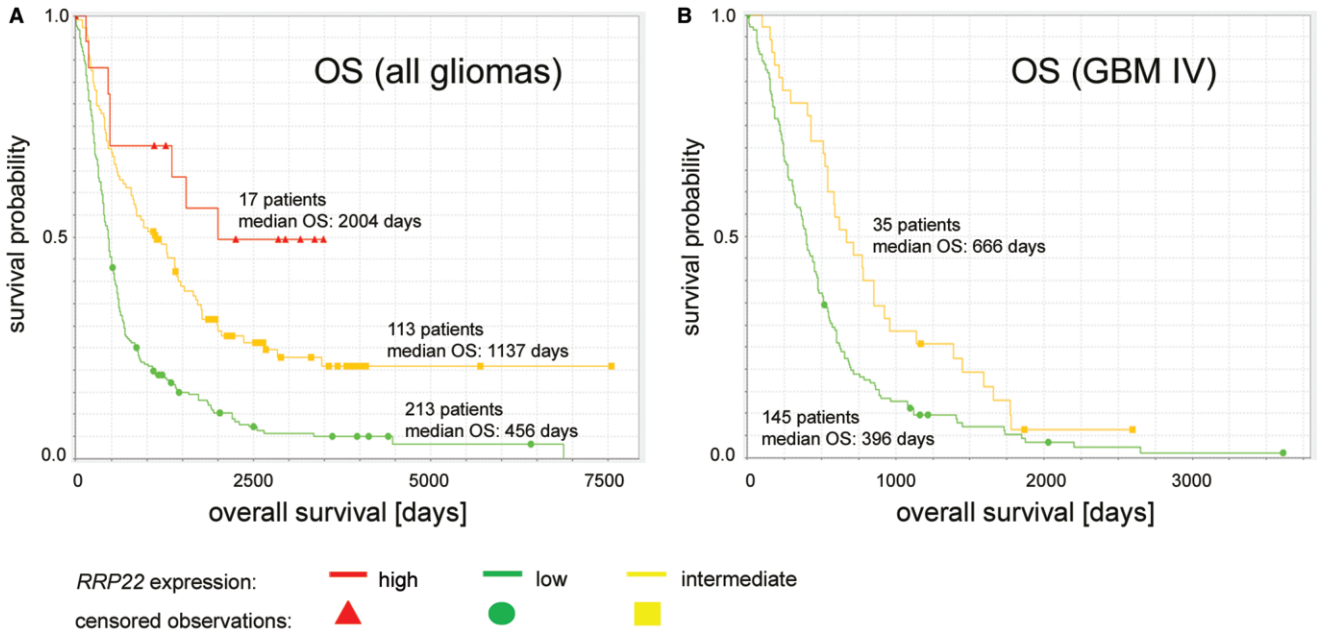

Figure 6. Kaplan–Meier survival plots of glioma patients in the REMBRANDT data set stratified for *RRP22* expression levels. (**A**) Note that overall survival (OS) is positively associated with the level of *RRP22* mRNA expression in a group of 343 patients diagnosed with diffusely infiltrating gliomas of different WHO grades. (**B**) Univariate survival correlation of 180 glioblastoma patients stratified for differences in *RRP22* expression levels revealed that higher *RRP22* transcripts levels are associated with longer OS. As only a single glioblastoma patient fell into the group of "high *RRP22* expression", for statistical comparisons we only utilized survival curves for low and intermediate *RRP22* expression levels.

RRP22 transcript levels, arguing for a causal relationship between *RRP22* 5′-CpG island methylation and decreased expression. In our primary tumor panel, there was only a trend toward significance for the correlation between *RRP22* methylation status and *RRP22* mRNA expression levels. In fact, several *RRP22* hypermethylated gliomas did not exhibit reduced *RRP22* transcript levels, which might be explained by the often high degree of cellular and molecular heterogeneity of these tumors. Given that *RRP22* hypermethylation in such cases may be restricted to a subset of tumor cells, expression might still be sustained from unmethylated tumor cell subpopulations or contaminating non-neoplastic cell populations, such as, for example, microglial cells. Similar pitfalls in the correlation of methylation and expression data when using lsyate-base approaches have been described for other hypermethylated genes, such as the O^6-methylguanine-DNA-methyltransferase (*MGMT*) gene (6).

More importantly, however, we found that *RRP22* hypermethylation could only explain for the reduced mRNA expression in a subset of tumor samples (30 out of 47 patients), suggesting that mechanisms in addition to CpG island methylation might contribute to the frequent silencing of *RRP22* in human gliomas. Our search for tumor-associated structural genetic alterations yielded only low frequencies of allelic losses at the *RRP22* locus on chromosome 22q12.2, while tumor-associated mutations were absent.

As histone modifications may serve as an important alternative mechanism of gene inactivation (10, 18), we treated glioblastoma cell lines *in vitro* with the histone deactylase inhibitor TSA, leading to an euchromatinization of gene promoters. Indeed, TSA treatment significantly increased the mRNA expression levels of *RRP22*, suggesting that histone modifications might contribute to the silencing of *RRP22* in gliomas. Chromatin-immunoprecipitation after TSA treatment corroborated a significant increase of *RRP22* promoter DNA bound to the acetylated histones H3 (H3ac) and H4 (H4ac). This finding was confirmed by ChIP in a separate subset of glioblastoma tissue samples. Three out of seven investigated primary glioblastomas showed a shift toward a heterochromatinization of the *RRP22* promoter relative to non-neoplastic brain tissue. This heterochromatinization of *RRP22* was found alone or in coincidence with *RRP22* 5'-CpG island methylation and in both settings associated with a marked downregulation of *RRP22* transcripts. Thus, histone modifications might serve as an additional cause of *RRP22* inactivation and either alone or in conjunction with *RRP22* 5'-CpG island hypermethylation account for the gene's frequent transcriptional downregulation in human gliomas.

RRP22 epigenetic inactivation did not reveal a significant association to other molecular alterations common in gliomas, namely *IDH1/2* mutations, allelic losses on 1p and 19q as well as p53 protein accumulation. This does not appear surprising given the fact that *RRP22* epigenetic inactivation neither spares or prefers primary glioblastomas nor occurs strikingly more often in either oligodendroglial or astrocytic neoplasms. Gliomas with *RRP22* epigenetic inactivation by promoter hypermethylation or histone modifications are thus not associated with a distinct group of gliomas characterized by one of the three investigated "classic" molecular alterations (*IDH1/2* mutation, 1p/19q deletion, p53 protein expression).

Publicly available data from the NIH REMBRANDT database are in accordance with our finding that *RRP22* expression

© 2011 The Authors; Brain Pathology © 2011 International Society of Neuropathology

decreases with an increasing malignancy grade of gliomas. More interestingly, Kaplan–Meier survival plots indicate a worse overall survival for patients whose tumors demonstrate low *RRP22* expression levels, both in a group of glioma patients of different WHO grades as well as in glioblastoma patients alone. These data strongly suggest that *RRP22* inactivation represents a negative prognostic factor in glioma patients.

In summary, we here present the first study systematically assessing the molecular aberrations and inactivation mechanisms of *RRP22* in primary human tumors. We uncovered that *RRP22* 5′-CpG island hypermethylation and/or histone modifications may underlie the frequent and prognostically unfavorable transcriptional downregulation of the *RRP22* gene in human gliomas.

ACKNOWLEDGMENTS

The authors would like to thank Nina Graffmann (Institute for Transplantation Diagnostics and Cell Therapeutics, Düsseldorf), Dr. Melanie Ruppel (German Cancer Research Center, Heidelberg) and Dr. Daniela Karra (Department of Neuropathology, Düsseldorf) for their valuable support in establishing the ChIP-Assays. Britta Friedensdorf is acknowledged for her skillful technical assistance and Joerg Felsberg for his support in scoring the p53 immunostains. This work was financially supported by grants from the German Cancer Aid (Max-Eder Junior Research Group Program, grant no. 107709 and 109426), the Research Commission of the Medical Faculty of the Heinrich Heine University Düsseldorf (grant no. 9772307) and the Academy of Sciences of Northrhine-Westfalia/Mercator Foundation (“Junges Kolleg”) (all to Markus J. Riemenschneider).

CONFLICT OF INTEREST STATEMENT

The authors have no conflict of interest to declare.

REFERENCES

1. Barski D, Wolter M, Reifenberger G, Riemenschneider MJ (2010) Hypermethylation and transcriptional downregulation of the TIMP3 gene is associated with allelic loss on 22q12.3 and malignancy in meningiomas. *Brain Pathol* **20**:623–631.
2. Bos JL (1989) Ras oncogenes in human cancer: a review. *Cancer Res* **49**:4682–4689.
3. Chen R, Yang L, Fang J, Huo L, Zhang M, Chen F *et al* (2011) RRP22: a novel neural tumor suppressor for astrocytoma. *Med Oncol* 2011 Jan 25. [Epub ahead of print].
4. Elam C, Hesson L, Vos MD, Eckfeld K, Ellis CA, Bell A *et al* (2005) RRP22 is a farnesylated, nucleolar, Ras-related protein with tumor suppressor potential. *Cancer Res* **65**:3117–3125.
5. Felsberg J, Erkwoh A, Sabel MC, Kirsch L, Fimmers R, Blaschke B *et al* (2004) Oligodendroglial tumors: refinement of candidate regions on chromosome arm 1p and correlation of 1p/19q status with survival. *Brain Pathol* **14**:121–130.
6. Felsberg J, Rapp M, Loeser S, Fimmers R, Stummer W, Goeppert M *et al* (2009) Prognostic significance of molecular markers and extent of resection in primary glioblastoma patients. *Clin Cancer Res* **15**:6683–6693.
7. Felsberg J, Wolter M, Seul H, Friedensdorf B, Goppert M, Sabel MC, Reifenberger G (2010) Rapid and sensitive assessment of the IDH1 and IDH2 mutation status in cerebral gliomas based on DNA pyrosequencing. *Acta Neuropathol* **119**:501–507.
8. Ino Y, Silver JS, Blazejewski L, Nishikawa R, Matsutani M, von Deimling A, Louis DN (1999) Common regions of deletion on chromosome 22q12.3-q13.1 and 22q13.2 in human astrocytomas appear related to malignancy grade. *J Neuropathol Exp Neurol* **58**:881–885.
9. Jiang Y, Matevossian A, Huang HS, Straubhaar J, Akbarian S (2008) Isolation of neuronal chromatin from brain tissue. *BMC Neurosci* **9**:42.
10. Kouzarides T (2007) Chromatin modifications and their function. *Cell* **128**:693–705.
11. Livak KJ, Schmittgen TD (2001) Analysis of relative gene expression data using real-time quantitative PCR and the 2(-delta delta C(T)) method. *Methods* **25**:402–408.
12. Louis DN, Ohgaki H, Wiestler OD, Cavenee WK, Burger PC, Jouvet A *et al* (2007) The 2007 WHO classification of tumours of the central nervous system. *Acta Neuropathol* **114**:97–109.
13. Mueller W, Nutt CL, Ehrich M, Riemenschneider MJ, von Deimling A, van den Boom D, Louis DN (2007) Downregulation of RUNX3 and TES by hypermethylation in glioblastoma. *Oncogene* **26**:583–593.
14. Newton HB (2003) Molecular neuro-oncology and development of targeted therapeutic strategies for brain tumors. Part 1: growth factor and Ras signaling pathways. *Expert Rev Anticancer Ther* **3**:595–614.
15. Riemenschneider MJ, Reifenberger J, Reifenberger G (2008) Frequent biallelic inactivation and transcriptional silencing of the DIRAS3 gene at 1p31 in oligodendroglial tumors with 1p loss. *Int J Cancer* **122**:2503–2510.
16. Sayagues JM, Tabernero MD, Maillo A (2007) [Cytogenetic alterations in meningioma tumors and their impact on disease outcome]. *Med Clin (Barc)* **128**:226–232.
17. Schagger H (2006) Tricine-SDS-PAGE. *Nat Protoc* **1**:16–22.
18. Schones DE, Zhao K (2008) Genome-wide approaches to studying chromatin modifications. *Nat Rev Genet* **9**:179–191.
19. Tepel M, Roerig P, Wolter M, Gutmann DH, Perry A, Reifenberger G, Riemenschneider MJ (2008) Frequent promoter hypermethylation and transcriptional downregulation of the NDRG2 gene at 14q11.2 in primary glioblastoma. *Int J Cancer* **123**:2080–2086.
20. Yin D, Ong JM, Hu J, Desmond JC, Kawamata N, Konda BM *et al* (2007) Suberoylanilide hydroxamic acid, a histone deacetylase inhibitor: effects on gene expression and growth of glioma cells *in vitro* and *in vivo*. *Clin Cancer Res* **13**:1045–1052.
21. Zucman-Rossi J, Legoix P, Thomas G (1996) Identification of new members of the Gas2 and Ras families in the 22q12 chromosome region. *Genomics* **38**:247–254.

SUPPORTING INFORMATION

Additional Supporting Information may be found in the online version of this article:

Table S1. Primers used for expression, mutation, methylation and ChIP analysis of *RRP22* and microsatellite analyses of the 22q12 locus spanning *RRP22*.

Please note: Wiley-Blackwell are not responsible for the content or functionality of any supporting materials supplied by the authors. Any queries (other than missing material) should be directed to the corresponding author for the article.

© 2011 The Authors; Brain Pathology © 2011 International Society of Neuropathology